Dielectric elastomer membranes undergoing inhomogeneous deformation

Tianhu He,[1,2] Xuanhe Zhao,[2] and Zhigang Suo[2,a)]
[1]*Department of Mechanics and Engineering Science and Key Laboratory of Mechanics on Western Disaster and Environment, College of Civil Engineering and Mechanics, Lanzhou University, Lanzhou, Gansu 730000, People's Republic of China*
[2]*School of Engineering and Applied Sciences, Harvard University, Cambridge, Massachusetts 02138, USA*

(Received 23 June 2009; accepted 22 September 2009; published online 29 October 2009)

Dielectric elastomers are capable of large deformation subject to an electric voltage and are promising for use as actuators, sensors, and generators. Because of large deformation, nonlinear equations of states, and diverse modes of failure, modeling the process of electromechanical transduction has been challenging. This paper studies a membrane of a dielectric elastomer deformed into an out-of-plane axisymmetric shape, a configuration used in a family of commercial devices known as the universal muscle actuators. The kinematics of deformation and charging, together with thermodynamics, leads to equations that govern the state of equilibrium. Numerical results indicate that the field in the membrane can be very inhomogeneous, and that the membrane is susceptible to several modes of failure, including electrical breakdown, loss of tension, and rupture by stretch. Care is needed in the design to balance the requirements of averting various modes of failure while using the material efficiently. © *2009 American Institute of Physics*.
[doi:10.1063/1.3253322]

I. INTRODUCTION

As a class of materials for electromechanical transduction, dielectric elastomers posses a unique combination of attributes: large deformation, fast response, high efficiency, low cost, and light weight.[1–3] These attributes make dielectric elastomers promising for applications as transducers in, for example, cameras, robots, and energy harvesters.[4–8] The essential part of such a transducer is a membrane of a dielectric elastomer. Subject to a voltage, the membrane reduces its thickness and expands its area, converting electrical energy into mechanical energy.

To deform an elastomer appreciably, the electric field needed scales as $E\sim\sqrt{\mu/\varepsilon}$, where μ is the elastic modulus of the elastomer and ε is the permittivity. Using representative values, $\mu=4\times10^5$ N/m^2 and $\varepsilon=4\times10^{-11}$ F/m, one finds that actuating a dielectric elastomer requires an enormous electric field, of the order of $E\sim10^8$ V/m. The intense electric field has major consequences in the design of transducers. The membrane nearly always operates on the verge of *electrical breakdown*, where the electric field may mobilize charged species in the elastomer to produce a path of electrical conduction. The membrane is also susceptible to an instability specific to deformable dielectrics. As the applied voltage is increased, the elastomer reduces its thickness so that the voltage induces an even higher electric field. The positive feedback between a thinner elastomer and a higher electric field may cause the elastomer to thin down drastically, resulting in *electromechanical instability*.[9,10] Furthermore, to avoid excessively high voltage in use, the membrane must be thin. For example, an electric field of 10^8 V/m in a 1 mm thick membrane requires a voltage of 10^5 V. The thin membrane, however, buckles under slight compressive stresses in its plane. Even for a pretensioned membrane, the applied voltage induces deformation, which may remove the tensile prestress, a condition known as *loss of tension*. Of course, when the polymer chains in the membrane are stretched severely, the membrane is susceptible to *rupture by stretch*.

While these modes of failure are known to limit the performance of dielectric elastomer transducers, few systematic studies have been reported.[11,12] Modeling dielectric elastomer transducers has been challenging due to the diverse modes of failure, as well as large deformation and nonlinear equations of states.[13–16] This paper explores these issues by studying a membrane of a dielectric elastomer deformed into an out-of-plane axisymmetric shape (Fig. 1), a configuration used in a family of commercial devices known as universal muscle actuators (UMAs), marketed by Artificial Muscle, Inc. While many other configurations have been proposed in literature, the focus on a particular configuration, such as the UMAs, may bring the benefits of standardization while still addressing a large range of early applications.[17,18] To focus our attention even further, this paper will be restricted to the fundamental issues of electromechanics of membranes. In particular, attention here will be placed on a single membrane, as illustrated in Fig. 1, rather than two membranes used in UMAs.

The study of axisymmetric deformation of membranes has a long tradition.[19,20] Also studied recently is the axisymmetric deformation of membranes subject to electromechanical loads.[21–23] In this paper, we use these analytical and computational tools to study various modes of failure. We combine the kinematics of axisymmetric deformation of membranes and the thermodynamics of elastic dielectrics. This approach follows the recent studies of elastic dielectrics.[24–26] Governing equations derived here recover those in Ref. 21 for an idealized material model and can

a)Electronic mail: suo@seas.harvard.edu.

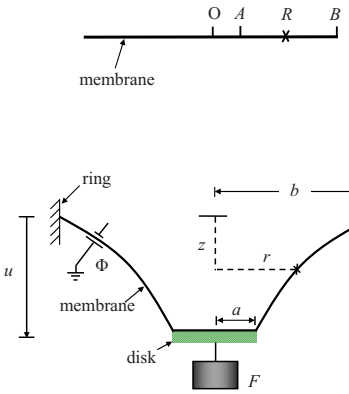

FIG. 1. (Color online) Schematic cross section of an actuator. A circular membrane of a dielectric elastomer is sandwiched between two compliant electrodes. (a) In the undeformed state, the membrane is of radius B and a particle of the membrane is at a distance A from the center O. Label a general particle of the membrane by the distance R of the particle from the center. (b) In the deformed state, the membrane is attached to a rigid circular disk of radius a and to a rigid circular ring of radius b, such that particle A moves to the place a and particle B moves to the place b. The ring is then held fixed, a force F is applied to the disk, and a voltage Φ is applied between the electrodes. In response to the applied load, the disk moves relative to the ring by a distance u, an amount of charge Q flows from one electrode to the other, and particle R moves to a place with coordinates $r(R)$ and $z(R)$.

accommodate more general material models. We then describe numerical results for the specific configuration illustrated in Fig. 1. We show that the field in the membrane can be highly inhomogeneous, such that a judicious design is needed to avert various modes of failure, while using the material efficiently.

II. STATE OF EQUILIBRIUM

Figure 1 illustrates the cross section of a membrane of a dielectric elastomer. A circular dielectric membrane is coated on both surfaces with compliant electrodes. In the undeformed state [Fig. 1(a)], the membrane is of thickness H and radius B. A specific particle of the membrane is at a distance A from the center O, and a general particle is at a distance R from the center. In the deformed state [Fig. 1(b)], the membrane is attached to a rigid disk of radius a and to a rigid ring of radius b such that particle A moves to the place a and particle B moves to the place b. When a force F is applied to the disk and a voltage Φ is applied between the two electrodes, the disk moves relative to the ring by a distance u, and an amount of charge Q flows from one electrode to the other. Meanwhile, the membrane deforms into an out-of-plane axisymmetric shape.

Following Ref. 19, we first examine the kinematics of deformation. In the deformed state [Fig. 1(b)], particle R moves to a place with coordinates r and z. The two functions, $r(R)$ and $z(R)$, fully describe the deformed shape and are subject to the following boundary conditions: $r(A)=a$, $r(B)=b$, $z(A)=u$, and $z(B)=0$. Consider the longitudinal stretch by examining two nearby particles, R and $R+dR$. In the deformed state, the two particles occupy places separated by $dr=r(R+dR)-r(R)$ and $dz=z(R+dR)-z(R)$. Let dl be the distance between the two particles when the membrane is in the deformed state and $\theta(R)$ be the slope of the vector connecting the two particles so that $dr=\cos\theta dl$, $dz=-\sin\theta dl$, and $(dl)^2=(dr)^2+(dz)^2$. The longitudinal stretch is defined by the distance between the two particles in the deformed state divided by that in the undeformed state, $\lambda_1=dl/dR$. In terms of the functions $r(R)$ and $z(R)$, the longitudinal stretch is

$$\lambda_1=\sqrt{\left(\frac{dr}{dR}\right)^2+\left(\frac{dz}{dR}\right)^2}. \tag{1}$$

Consider the latitudinal stretch by examining a circle of material particles of perimeter $2\pi R$ in the undeformed state. In the deformed state, the circle of particles occupies a circle of places of perimeter $2\pi r(R)$. Thus, the latitudinal stretch is

$$\lambda_2=\frac{r}{R}. \tag{2}$$

To characterize the kinematics of charging, we use nominal electric displacement (see Refs. 26 and 25 for more general discussion). In the deformed state, let $\tilde{D}$ be the nominal electric displacement, namely, the electric charge on an element of an electrode in the deformed state divided by the area of the element in the undeformed state. Consequently, in the deformed state, the total electric charge on the electrode is

$$Q=2\pi\int\tilde{D}RdR. \tag{3}$$

Together, λ_1, λ_2, and $\tilde{D}$ are the three kinematic variables that characterize the state of an element of the membrane.

The membrane is a thermodynamic system, taken to be held at a constant temperature. Let W be the Helmholtz free energy of an element of the dielectric in the deformed state divided by the volume of the element in the undeformed state. Consequently, the Helmholtz free energy of the entire membrane in the deformed state is $2\pi H\int WRdR$. We stipulate that the free-energy density is a function of the three kinematic variables, $W(\lambda_1,\lambda_2,\tilde{D})$.

When the kinematic variables vary by small amounts, the free-energy density varies by

$$\delta W=s_1\delta\lambda_1+s_2\delta\lambda_2+\tilde{E}\delta\tilde{D}. \tag{4}$$

This equation defines the three partial differential coefficients,

$$s_1=\frac{\partial W(\lambda_1,\lambda_2,\tilde{D})}{\partial\lambda_1}, \tag{5a}$$

$$s_2=\frac{\partial W(\lambda_1,\lambda_2,\tilde{D})}{\partial\lambda_2}, \tag{5b}$$

$$\tilde{E}=\frac{\partial W(\lambda_1,\lambda_2,\tilde{D})}{\partial\tilde{D}}. \tag{5c}$$

These partial differential coefficients can be readily interpreted from Eq. (4): s_1 is the longitudinal nominal stress, s_2

is the latitudinal nominal stresses, and $\tilde{E}$ is the nominal electric field. Once a free-energy function $W(\lambda_1,\lambda_2,\tilde{D})$ is prescribed for a given material, Eq. (5) constitutes the equations of states.

We now combine the kinematics and thermodynamics to derive the equations that govern the state of equilibrium. This approach avoids the introduction of the nebulous notion of electric body force (see Ref. 26 for further discussion). When the rigid disk moves by a small distance δu, the applied force does work $F\delta u$. When a small amount of charge δQ flows from one electrode to the other, the applied voltage does work $\Phi\delta Q$. In a state of equilibrium, thermodynamics dictates that for arbitrary variation in the system, the change in the Helmholtz free energy of the membrane should equal the sum of the work done by the applied force and the applied voltage, namely,

$$2\pi H\int_A^B \delta W R dR = F\delta u + \Phi\delta Q. \tag{6}$$

Let the membrane be in a state of equilibrium characterized by $r(R)$, $z(R)$, and $\tilde{D}(R)$, and let the state undergo a small variation characterized by $\delta r(R)$, $\delta z(R)$, and $\delta\tilde{D}(R)$. From Eq. (1), we obtain the associated variation in the longitudinal stretch

$$\delta\lambda_1 = \cos\theta\frac{d(\delta r)}{dR} - \sin\theta\frac{d(\delta z)}{dR}.$$

Using Eq. (4) and integrating by parts, we obtain that

$$\int_A^B \delta W R dR = (Rs_1\cos\theta\delta r - Rs_1\sin\theta\delta z)\Big|_A^B + \int_A^B\left\{\left[-\frac{d(Rs_1\cos\theta)}{dR}+s_2\right]\delta r + \frac{d(Rs_1\sin\theta)}{dR}\delta z + R\tilde{E}\delta\tilde{D}\right\}dR. \tag{7}$$

Comparing Eqs. (6) and (7) and recalling that $\delta r(R)$, $\delta z(R)$, and $\delta\tilde{D}(R)$ are independent variations, we obtain that

$$2\pi HRs_1\sin\theta = F, \tag{8}$$

$$\frac{d(Rs_1\cos\theta)}{dR} = s_2, \tag{9}$$

$$H\tilde{E} = \Phi. \tag{10}$$

Equations (8) and (9) can also be obtained by balancing forces in the directions of z and r, respectively, as done in literature.[20] Equation (10) recovers the definition of the nominal electric field.

III. MATERIAL MODEL

To carry out numerical calculations, we need to prescribe an explicit form of the free-energy function $W(\lambda_1,\lambda_2,\tilde{D})$. Here, we adopt a material model, called the ideal dielectric elastomer, where the dielectric behavior is liquidlike, unaffected by deformation.[27] Specifically, the true electric displacement is linear in the true electric field, and the permittivity is independent of deformation. This material model seems to describe some experimental data[28] but is inconsistent with other experimental data.[16] Nevertheless, this model has been used almost exclusively in previous analyses of dielectric elastomers. For a model of nonideal dielectric elastomers, see Refs. 24 and 29. In what follows, we develop results for the ideal dielectric elastomer.

The elastomer is assumed to be incompressible so that the stretch in the thickness direction of the membrane, λ_3, relates to the longitudinal and latitudinal stretches as $\lambda_3=1/(\lambda_1\lambda_2)$. The thickness of the membrane is H in the undeformed state and is $\lambda_3 H=H/(\lambda_1\lambda_2)$ in the deformed state. By definition, the true electric field E is the voltage divided by the thickness of the membrane in the deformed state so that $E=\lambda_1\lambda_2\Phi/H=\lambda_1\lambda_2\tilde{E}$. The true electric displacement D is defined as the charge in the deformed state divided by the area of the membrane in the deformed state so that $D=\tilde{D}/(\lambda_1\lambda_2)$.

For the ideal dielectric elastomer, we assume that the free-energy density takes the form[27]

$$W = \frac{\mu}{2}(\lambda_1^2+\lambda_2^2+\lambda_3^2-3)+\frac{1}{2}\varepsilon E^2. \tag{11}$$

The first term is the elastic energy, where μ is the small strain shear modulus. The elastomer is taken to be a network of long and flexible polymers obeying the Gaussian statistics so that the elastic behavior of the elastomer is neo-Hookean. The second term is the dielectric energy, where ε is the permittivity. For the ideal dielectric elastomer, the dielectric behavior is liquidlike, unaffected by the deformation. Specifically, the true electric displacement relates to the true electric field as $D=\varepsilon E$, the dielectric energy per unit volume is $\varepsilon E^2/2$, and the permittivity ε is a constant independent of deformation.

To obtain the equations of states from Eq. (5), we need to express the free energy W as a function of $(\lambda_1,\lambda_2,\tilde{D})$. Recall the condition of incompressibility, $\lambda_3=1/(\lambda_1\lambda_2)$, and the assumption of the liquidlike dielectric behavior, $E=D/\varepsilon=\tilde{D}/(\varepsilon\lambda_1\lambda_2)$. Equation (11) is rewritten as

$$W(\lambda_1,\lambda_2,\tilde{D}) = \frac{\mu}{2}(\lambda_1^2+\lambda_2^2+\lambda_1^{-2}\lambda_2^{-2}-3)+\frac{\tilde{D}^2}{2\varepsilon}\lambda_1^{-2}\lambda_2^{-2}. \tag{12}$$

Inserting Eq. (12) into Eq. (5), we obtain the following equations of states:

$$s_1 = \mu(\lambda_1-\lambda_1^{-3}\lambda_2^{-2})-\frac{\tilde{D}^2}{\varepsilon}\lambda_1^{-3}\lambda_2^{-2}, \tag{13a}$$

$$s_2 = \mu(\lambda_2-\lambda_2^{-3}\lambda_1^{-2})-\frac{\tilde{D}^2}{\varepsilon}\lambda_2^{-3}\lambda_1^{-2}, \tag{13b}$$

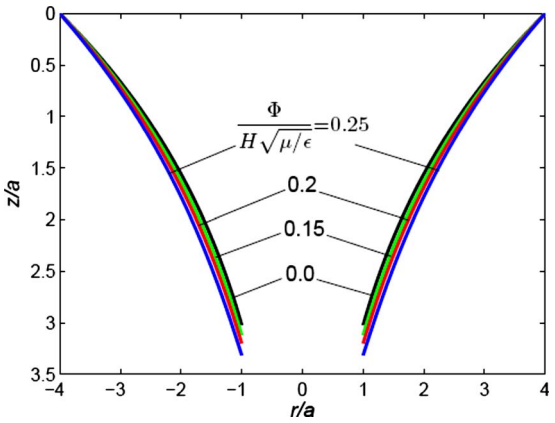

FIG. 2. (Color online) Deformed shapes of the membrane when the actuator is subject to a fixed force and several levels of voltage.

$$\tilde{E} = \frac{\tilde{D}}{\varepsilon}\lambda_1^{-2}\lambda_2^{-2}. \tag{13c}$$

Recall that the true stresses σ_1 and σ_2 relate to the nominal stresses as $\sigma_1 = \lambda_1 s_1$ and $\sigma_2 = \lambda_2 s_2$. We rewrite Eq. (13) in terms of the true quantities,

$$\sigma_1 = \mu(\lambda_1^2 - \lambda_1^{-2}\lambda_2^{-2}) - \varepsilon E^2, \tag{14a}$$

$$\sigma_2 = \mu(\lambda_2^2 - \lambda_2^{-2}\lambda_1^{-2}) - \varepsilon E^2, \tag{14b}$$

$$D = \varepsilon E. \tag{14c}$$

These equations are readily interpreted. For example, the first term in Eq. (14a) is the contribution to the stress due to the change in entropy associated with the stretch of the polymer network, and the second term is the contribution to the stress due to the applied voltage. Equation (14) in various forms has been used in previous analyses.[13,21]

IV. NUMERICAL RESULTS AND DISCUSSIONS

The theory presented above results in coupled nonlinear differential and algebraic equations, which we solve numerically (see the Appendix for an outline of the method). This section describes the results and discusses their implications. As discussed above, the membrane is a thermodynamic system of two generalized coordinates: the displacement u of the rigid disk and the amount of charge Q on either electrode. The respective work-conjugate loading parameters are the applied force F and the applied voltage Φ. In presenting the results, we normalize the four variables into dimensionless forms: u/a, $Q/(2\pi a^2\sqrt{\varepsilon\mu})$, $F/(2\pi aH\mu)$, and $\Phi/(H\sqrt{\mu/\varepsilon})$.

Unless otherwise stated, we fix the applied force to $F/(2\pi aH\mu)=2$ and vary the voltage applied. In designing a device using the configuration in Fig. 1, three dimensionless parameters can be varied: a/A, b/B, and b/a. We first fix the three parameters to specific values, $a/A=b/B=1.2$ and $b/a=4$.

Figure 2 plots the cross section of the deformed shapes of the membrane. As the voltage increases, the membrane expands its area and lowers the disk. Observe that the cross section of the membrane is curved due to the deformation in three dimensions.

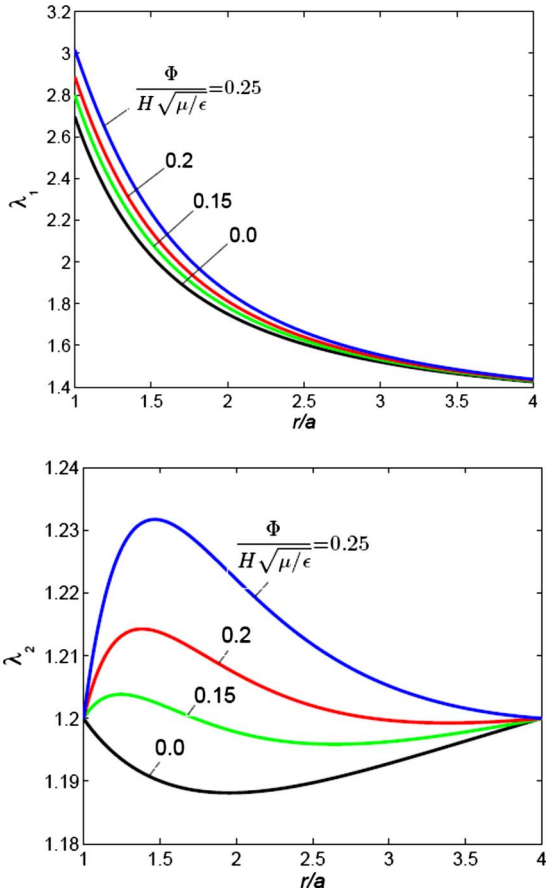

FIG. 3. (Color online) The distributions of stretches in the membrane.

Figure 3 plots the distribution of the stretches λ_1 and λ_2 in the membrane. As expected, both stretches increase with the voltage. At a fixed voltage, the longitudinal stretch λ_1 is largest at the inner end of the membrane and monotonically reduces to the smallest value at the outer end. The latitudinal stretch λ_2 is held at the prescribed values at the two ends by the disk and the ring, and reaches maximum in the middle region of the membrane.

Figure 4 plots the distribution of the true stresses in the membrane. To balance the applied force in the z direction [Eq. (8)], the longitudinal stress σ_1 is always tensile. The latitudinal stress σ_2, however, can become compressive when the applied voltage is large. This loss of tension may cause the membrane to buckle. Figure 4 shows that the stresses are inhomogeneous in the membrane, and the loss of tension is expected to occur first at the inner end of the membrane.

Figure 5 plots the distribution of the true electric field in the membrane. Recall that the applied voltage Φ is homogenous in the membrane. Consequently, the true electric field, $E=\Phi\lambda_1\lambda_2/H$, scales with $\lambda_1\lambda_2$. As shown in Fig. 3, the two stretches reach maximum in different regions in the membrane. Figure 5 shows that E increases monotonically from the outer end of the membrane to the inner end. Assume that electrical breakdown occurs when the true electric field ex-

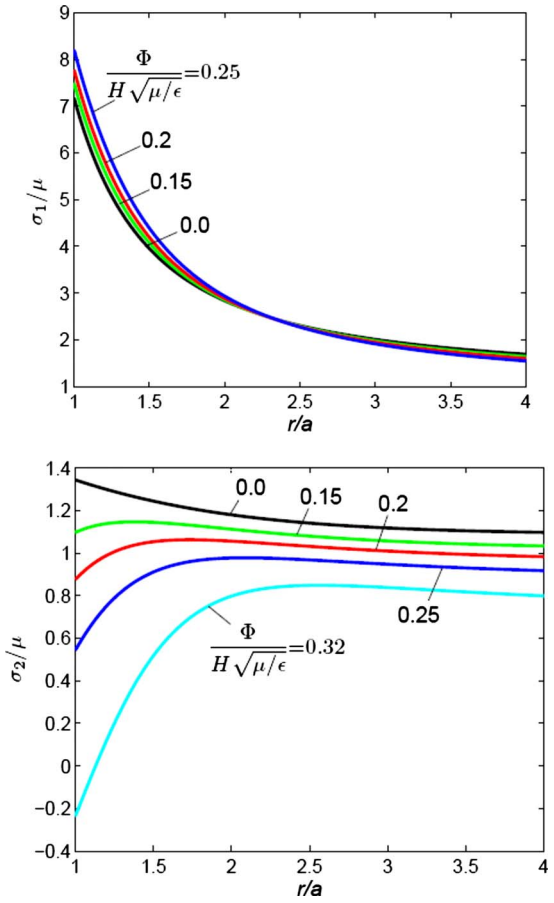

FIG. 4. (Color online) The distributions of true stresses in the membrane.

ceeds a critical value. Consequently, we expect that the electrical breakdown occurs at the inner end of the membrane when the voltage is too high.

Figure 6 plots the relation between the voltage and the displacement of the rigid disk. The range of the displacement corresponds to the range of actuation of the device. Figure 7 plots the relation between the voltage and the electric charge on either electrode. The area under this curve corresponds to the work done by the voltage.

Figure 8 shows the plane whose axes are the two generalized coordinates: the displacement of the disk and the charge induced on either electrode. A point on the plane represents a state of the transducer, and a curve on the plane represents a path of an electromechanical process. Figure 8 plots several paths of constant applied force and paths of constant applied voltage.

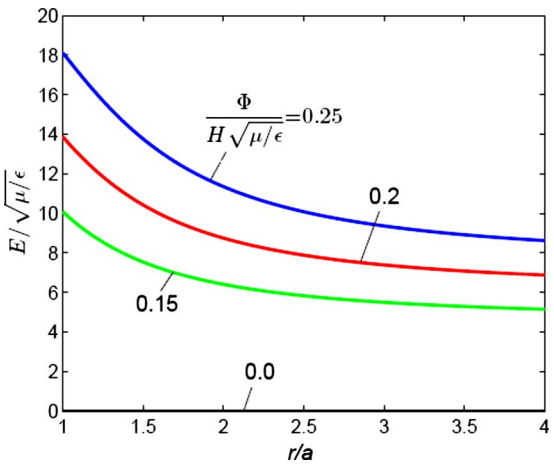

FIG. 5. (Color online) The distributions of true electric field in the membrane.

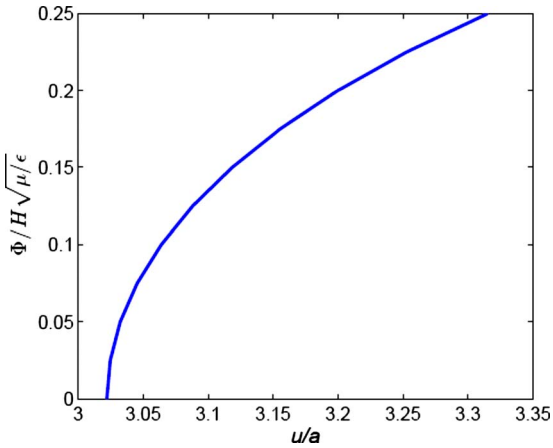

FIG. 6. (Color online) The relation between the applied voltage and the displacement of the disk.

As mentioned previously, the transducer has three parameters of design: a/A, b/B, and b/a. These parameters may be varied to modify the performance of the transducer. As an example, Fig. 9 plots the relations between the applied voltage and u/u_0 by varying a/A and b/B, while retaining $b/a=4$. Here, u is the displacement of the disk when the membrane is subject to a voltage and u_0 is the displacement of the disk when the membrane is subject to no voltage. At a fixed voltage, u/u_0 increases with $a/A=b/B$.

In addition to the cases where $a/A=b/B$, Fig. 9 also includes a case when $a/A=1.1$ and $b/B=1.8$. Figure 10 gives the distributions of the true electric field when $a/A=1.1$ and $b/B=1.8$. In this case, the true electric field in the membrane is nearly uniform.

As seen above, the various fields in the membrane are inhomogeneous. Consequently, some regions of the membrane may be on the verge of failure, while other regions are

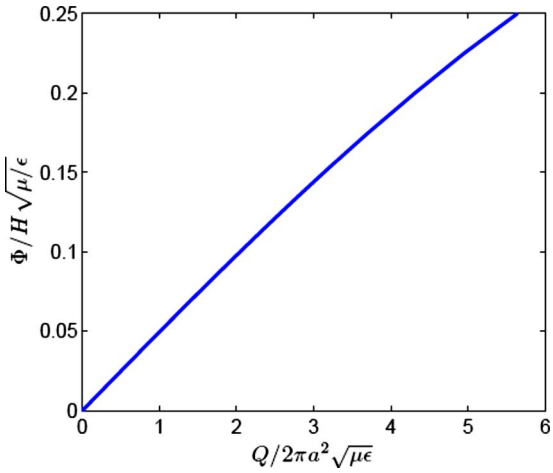

FIG. 7. (Color online) The relation between the applied voltage and the amount of electric charge on either electrode.

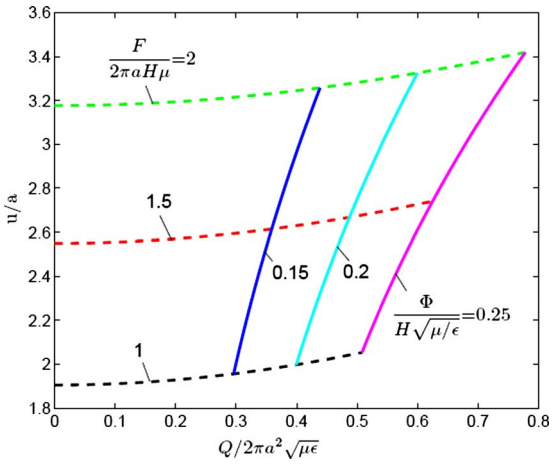

FIG. 8. (Color online) The actuator may be regarded as a thermodynamic system of two degrees of freedom, characterized by the generalized coordinates: the displacement of the disk and the charge induced on either electrode. Their respective work-conjugate generalized forces are the mechanical force applied to the disk and the electric voltage applied across the membrane. A point on the plane spanned by the two generalized coordinates represents a state of the actuator. A curve in the plane represents a path of actuation. Plotted in the plane are curves of constant applied force and curves of constant applied voltage.

still far below the capacity. This uneven distribution of the fields leads to an inefficient use of the material. However, once a particular device is selected and criteria for failure are specified, one can make judicious choice of the parameters of the design (e.g., a/A, b/B, and b/a) such that the material is used efficiently and various modes of failure are averted. Such an exercise of design is beyond the scope of this paper, but the method developed here should play an important role.

V. CONCLUDING REMARKS

To produce large deformation, a membrane is usually subject to an intense electric field and is susceptible to various modes of failure. Because the field in the membrane is inhomogeneous, the membrane may fail at a single point of high field, while the rest of the membrane operates much below its full capacity. This paper illustrates these issues by analyzing a configuration used in a family of commercial devices. We combine the kinematics of axisymmetric deformation with the thermodynamics of electromechanical interaction and obtain the governing equations for the inhomogeneous state of equilibrium. Numerical results illustrate several potential modes of failure, including electrical breakdown, loss of tension, and rupture by stretch. The approach can be used to optimize the design of electromechanical transducers for specific applications.

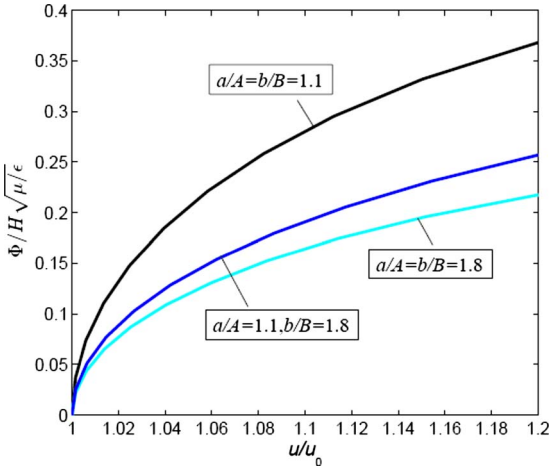

FIG. 9. (Color online) The relations of the applied voltages vs the ratio u/u_0 under several different a/A and b/B.

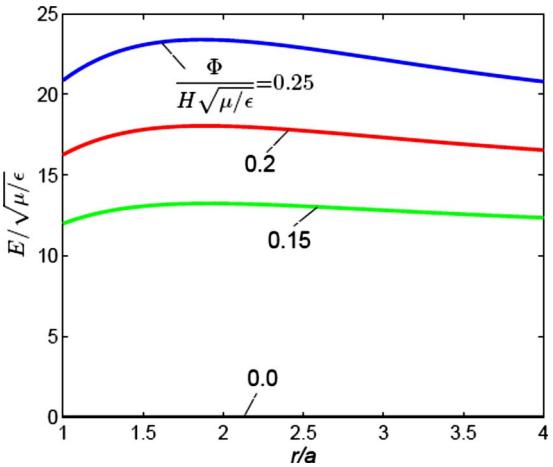

FIG. 10. (Color online) The distributions of true electric field in the membrane when $a/A=1.1$ and $b/B=1.8$.

ACKNOWLEDGMENTS

This work was supported by the National Science Foundation through a project on Large Deformation and Instability in Soft Active Materials. The visit of T.H. to Harvard University is sponsored by the Ministry of Education of the People's Republic of China. T.H. also acknowledges the support of the National Natural Science Foundation of China (Grant No. 10602021) and the Chinese Postdoctoral Science Foundation (Grant No. 20060400209). X.Z. acknowledges the support of the Founder's Prize, through the American Academy of Mechanics, sponsored by the Robert M. and Mary Haythornthwaite Foundation.

APPENDIX: COUPLED DIFFERENTIAL AND ALGEBRAIC EQUATIONS

Rewrite Eq. (1) as

$$\frac{dr}{dR} = \lambda_1 \cos\theta. \tag{A1}$$

A combination of Eqs. (8) and (9) gives

$$\frac{d\theta}{dR} = -\frac{s_2}{s_1 R}\sin\theta. \tag{A2}$$

The stresses in Eq. (A2) are expressed using Eqs. (13a) and (13b), which, in turn, are expressed as functions of r, λ_1, and Φ by using Eqs. (2), (10), and (13c). Rewrite the algebraic equation (8) as

$$\left[1-\left(\frac{\Phi r}{R}\right)^2\right]\lambda_1^4-\frac{F}{R\sin\theta}\lambda_1^3-\left(\frac{R}{r}\right)^2=o. \tag{A3}$$

In writing Eq. (A3), we have normalized F and Φ.

Once the force F and the voltage Φ are prescribed, the ordinary differential equations (A1) and (A2), together with the algebraic equation (A3), govern the three functions $r(R)$, $\theta(R)$, and $\lambda_1(R)$, subject to the boundary conditions $r(A)=a$ and $r(B)=b$. The boundary value problem is solved by using the shooting method. Once $r(R)$ are $\theta(R)$ are solved, the function $z(R)$ is determined by integrating $dz=-\tan\theta dr$, subject to the initial condition $z(B)=o$. We have checked our numerical results with those in Ref. 20 for the special case when the disk is moved by the applied force in the absence of the voltage.

[1] R. Pelrine, R. Kornbluh, Q. B. Pei, and J. Joseph, Science **287**, 836 (2000).
[2] R. E. Pelrine, R. D. Kornbluh, and J. P. Joseph, Sens. Actuators, A **64**, 77 (1998).
[3] F. Carpi, D. D. Rossi, R. Kornbluh, R. Pelrine, and P. Sommer-Larsen, *Dielectric Elastomers as Electromechanical Transducers: Fundamentals, Materials, Devices, Models and Applications of an Emerging Electroactive Polymer Technology* (Elsevier, Oxford, 2008).
[4] A. Wingert, M. D. Lichter, and S. Dubowsky, IEEE/ASME Trans. Mechatron. **11**, 448 (2006).
[5] Y. M. Liu, K. L. Ren, H. F. Hofmann, and Q. M. Zhang, IEEE Trans. Ultrason. Ferroelectr. Freq. Control **52**, 2411 (2005).
[6] J. Q. Xia, Y. R. Ying, and S. H. Foulger, Adv. Mater. (Weinheim, Ger.) **17**, 2463 (2005).
[7] Y. Bar-Cohen, J. Spacecr. Rockets **39**, 822 (2002).
[8] G. Kofod, W. Wirges, M. Paajanen, and S. Bauer, Appl. Phys. Lett. **90**, 081916 (2007).
[9] K. H. Stark and C. G. Garton, Nature (London) **176**, 1225 (1955).
[10] X. H. Zhao and Z. G. Suo, Appl. Phys. Lett. **91**, 061921 (2007).
[11] J. S. Plante and S. Dubowsky, Int. J. Solids Struct. **43**, 7727 (2006).
[12] M. Moscardo, X. Zhao, Z. Suo, and Y. Lapusta, J. Appl. Phys. **104**, 093503 (2008).
[13] M. Wissler and E. Mazza, Smart Mater. Struct. **14**, 1396 (2005).
[14] M. Wissler and E. Mazza, Sens. Actuators, A **120**, 184 (2005).
[15] M. Wissler and E. Mazza, Sens. Actuators, A **134**, 494 (2007).
[16] M. Wissler and E. Mazza, Sens. Actuators, A **138**, 384 (2007).
[17] N. Bonwit, J. Heim, M. Rosenthal, C. Duncheon, and A. Beavers, Proc. SPIE **6168**, 39 (2008).
[18] C. Duncheon, in *Dielectric Elastomers as Electromechanical Transducers: Fundamentals, Materials, Devices, Models and Applications of an Emerging Electroactive Polymer Technology*, edited by F. Carpi, D. D. Rossi, R. Kornbluh, R. Pelrine, and P. Sommer-Larsen (Elsevier, Oxford, 2008), Vol. 29.
[19] J. E. Adkins and R. S. Rivlin, Philos. Trans. R. Soc. London, Ser. A **244**, 505 (1952).
[20] T. E. Tezduyar, L. T. Wheeler, and L. Graux, Int. J. Non-Linear Mech. **22**, 61 (1987).
[21] N. Goulbourne, E. Mockensturm, and M. Frecker, ASME Trans. J. Appl. Mech. **72**, 899 (2005).
[22] E. M. Mockensturm and N. Goulbourne, Int. J. Non-Linear Mech. **41**, 388 (2006).
[23] N. C. Goulbourne, E. M. Mockensturm, and M. I. Frecker, Int. J. Solids Struct. **44**, 2609 (2007).
[24] R. M. McMeeking and C. M. Landis, Trans. ASME, J. Appl. Mech. **72**, 581 (2005).
[25] A. Dorfmann and R. W. Ogden, Acta Mech. **174**, 167 (2005).
[26] Z. G. Suo, X. H. Zhao, and W. H. Greene, J. Mech. Phys. Solids **56**, 467 (2008).
[27] X. H. Zhao, W. Hong, and Z. G. Suo, Phys. Rev. B **76**, 134113 (2007).
[28] G. Kofod, P. Sommer-Larsen, R. Kronbluh, and R. Pelrine, J. Intell. Mater. Syst. Struct. **14**, 787 (2003).
[29] X. H. Zhao and Z. G. Suo, J. Appl. Phys. **104**, 123530 (2008).